FEBS Letters 376 (1995) 216–220 FEBS 16357

Binding of the growth factor glycyl-L-histidyl-L-lysine by heparin

Dallas L. Rabenstein*, Jan M. Robert**, Siva Hari

Department of Chemistry, University of California at Riverside, Riverside, CA 92521, USA

Received 22 July 1995; revised version received 16 October 1995

Abstract Evidence is presented that the growth factor glycyl-histidyl-lysine (GHK) binds to heparin, and the interaction has been characterized by [^{1}H]NMR spectroscopy. ^{1}H chemical shifts indicate that GHK interacts with both the carboxylic acid and the carboxylate forms of heparin. The chemical shift data are consistent with a weak delocalized binding of the triprotonated (ImH^+, $GlyNH_3^+$, $LysNH_3^+$) form of GHK by the carboxylic acid form of heparin. As the pD is increased and the carboxylic acid groups are titrated, chemical shift data indicate that ammonium groups of GHK are hydrogen bonded to heparin carboxylate groups, while the histidyl imidazolium ring occupies the imidazolium-binding site of heparin. Evidence for site-specific binding includes displacement of chemical shift titration curves for heparin to lower pD, increased shielding of specific heparin protons by the imidazolium ring current and displacement of chemical shift titration curves for GHK to higher pD. Specific binding constants were determined for binding of the (ImH^+, $GlyNH_3^+$), $LysNH_3^+$), (ImH^+, $GlyNH_2$, $LysNH_3^+$) and (Im, $GlyNH_3^+$, $LysNH_3^+$) forms of GHK by the carboxylate form of heparin from chemical shift vs. pD titration data.

Key words: Glycyl-histidyl-lysine; Heparin; ^{1}H NMR; Growth factor

1. Introduction

The tripeptide growth factor glycyl-L-histidyl-L-lysine (GHK) was first isolated from human plasma in 1973 [1]. Since then, it has been shown to have a wide range of biological activities [2]. GHK stimulates the growth or enhances the viability of several types of cultured cells and organisms, including neuronal cells [3,4], lymphocytes [5], hepatocytes [1,6], Ascaris suum and Litomosoides carnii larvae [7,9], and the human tumor cell lines KB and HeLa [10]. GHK is a chemoattractant for capillary endothelial cells and mast cells [2,11,12]. Rapidly growing cells produce GHK or a similar peptide, and recent work suggests a role for GHK or its copper complex (GHK-Cu) in the processes of wound healing and tissue repair [2]. GHK-Cu accelerates the healing or closure of superficial wounds in rats, pigs and mice [2], and stimulates the accumulation of connective tissue in rat wounds [13,14].

Even though GHK and its copper complex have a wide range of biological activity, little is known about their specific interactions with biological macromolecules. Many polypeptide cytokines, including peptide growth factors, bind to the glycosaminoglycan heparin [15], and presumably to the closely related heparan sulfate part of cell surface heparan sulfate proteoglycans. In heparan sulfate, there are approximately equal numbers of N-sulfated and N-acetylated glucosamine residues, arranged predominantly in segregated 'block-wise' distributions [15,16]. Thus, heparin is considered to be a valid functional analog for binding to the heparin-like segments of heparan sulfate [16].

In this paper, we report that GHK binds to the glycosaminoglycan heparin; the binding interaction has been characterized by [^{1}H]NMR spectroscopy and is shown to involve the N-terminal glycyl ammonium, the histidyl imidazolium and the lysine ammonium groups, with the imidazolium group interacting site specifically with the imidazolium-binding site on heparin [17].

2. Materials and methods

Beef lung heparin (sodium salt) (153 USP U/mg, 16–17 kDa) and glycyl-histidyl-lysine were obtained from Sigma. NMR measurements were made on D_2O solutions containing heparin, GHK and heparin plus GHK. Heparin concentrations are expressed in terms of the concentration of the repeating disaccharide unit. Solution pD was adjusted with concentrated solutions of DCl and NaOD in D_2O. pD was measured using microcombination electrodes whose response was calibrated with certified standard buffer solutions; pH meter readings were converted to pD using the equation $pD = pH_{meter\ reading} + 0.40$ [18].

[^{1}H]NMR spectra were measured at 500 MHz and 37°C with a Varian VXR-500S NMR spectrometer. The residual HOD resonance was suppressed by selective presaturation for 1–2 s. before application of the non-selective observation pulse. ^{1}H chemical shifts were measured relative to the resonance for the methyl protons of internal *t*-butyl alcohol (δ = 1.2365 ppm) or 2,2-dimethyl-2-silapentane-5-sulfonate (DSS, δ = 0.0 ppm).

Non-linear least squares calculations were done with the program Scientist from MicroMath Scientific Software.

3. Results and discussion

Heparin is a negatively charged polysaccharide, comprised largely of repeating sequences of the trisulfated disaccharide {(1→4)-2-*O*-sulfo-α-L-idopyranosyluronic acid-(1→4)-2-deoxy-2-sulfamido-6-*O*-sulfo-α-D-glucopyranose} or (IdoA-2S)-(1→4)-($GlcNSO_3$-6S), shown below with the iduronic acid residue (the I ring) in the $^1C_4$ conformation and the glucosamine (the A ring) in the $^4C_1$ conformation. Because of its high negative charge density, many biological molecules, including histamine and many peptides and proteins [15,17], bind to heparin. The binding mechanism may be either delocalized (territorial) or site specific electrostatic interactions between anionic sites on heparin and cationic sites on the biological molecules [15].

The growth factor glycyl-histidyl-lysine has three potential sites for interaction with heparin: the glycyl ammonium group, the histidyl imidazolium group and the lysine ammonium group. Evidence for the binding of GHK by heparin was

*Corresponding author.

***Present address:* Department of Chemistry, University of South Florida, Tampa, FL 33620, USA.

SSDI 0014-5793(95)01286-9

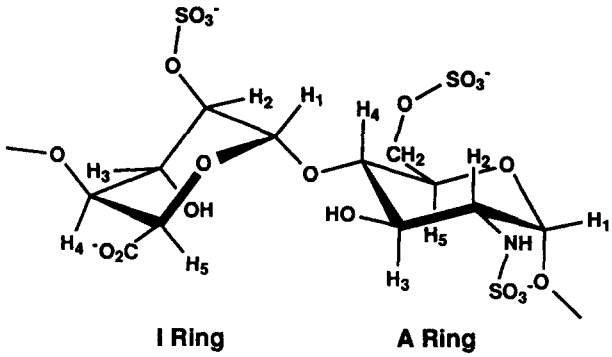

Scheme 1.

obtained from ^{1}H chemical shift data measured as a function of pD for heparin, the peptide and heparin plus peptide.

Chemical shift vs. pD data for the I5 and A3 protons of heparin are presented in Fig. 1 for free heparin and for heparin plus GHK at a 2.7:1 ratio. Chemical shift data are presented in Fig. 2 for the glycyl CH_2 and histidyl C2H protons and in Fig. 3 for the lysine ε-CH_2 protons of free GHK and of GHK plus heparin. The 2.8–5.5 ppm portion of representative spectra of solutions containing GHK plus heparin, with the resonances plotted in Figs. 1–3 identified, are presented in Fig. 4. The data in Figs. 1–3 establish that heparin binds GHK, that exchange of both GHK and heparin between their free and bound states is fast on the NMR time scale, and that the nature of the binding interaction is pD-dependent. Displacement of resonances for the Hep-A3, His-C2H, Gly-CH_2 and Lys ε-CH_2 protons at low pD indicates binding, presumably by non-specific electrostatic interactions between GHK and anionic sites on heparin. As the pD is increased over the range of 3–7 and the carboxylic acid group of the iduronic acid residue is titrated, the I5 resonance for free heparin (curve C in Fig. 1) shifts upfield; a pK_A of 5.49 ± 0.04 was obtained from the I5 chemical shift vs. pD data for free heparin. An apparent pK_A of 4.70 ± 0.03 was obtained from the data in the presence of GHK (curve D in Fig. 1). Displacement of the Hep-I5 chemical shift titration curve to lower pD indicates a specific interaction between the heparin carboxylate sites and GHK, as described by the following equilibria:

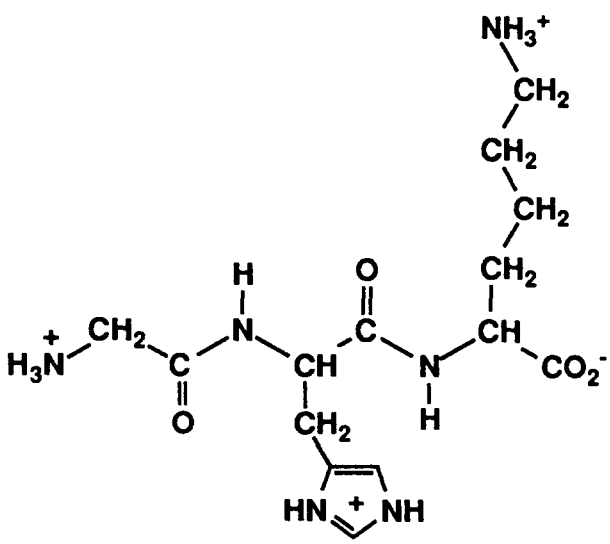

Scheme 2.

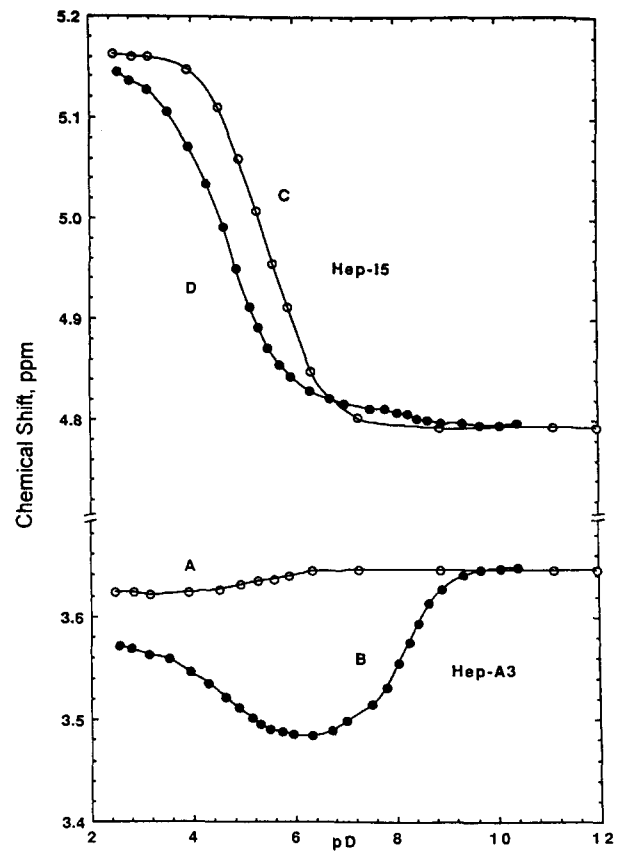

Fig. 1. Chemical shifts of resonances for the A3 and I5 protons of heparin as a function of pD; assignments are given on the structural formula of heparin. Curves A and C are for 12.3 mM sodium heparinate; curves B and D are for a solution of 13.7 mM sodium heparinate+5.1 mM GHK. Both solutions contain ~50 mM Na^+ from the sodium heparinate.

$$HepCO_2H \rightleftharpoons HepCO_2^- + H^+ \quad (1)$$

$$HepCO_2^- + H_3A^{2+} \rightleftharpoons HepCO_2^- - H_3A^{2+} \quad (2)$$

where H_3A^{2+} represents the triprotonated (ImH^+, $GlyNH_3^+$, $LysNH_3^+$) form of GHK. Formation of the $HepCO_2^-$–H_3A^{2+} complex has the effect of shifting the deprotonation equilibrium to the right.

The A3 resonance for free heparin (curve A) also shows a small change in chemical shift when the heparin carboxylic acid group is titrated due to a change in conformation across the (GlcNSO$_3$-6S)-(1→4)-(IdoA-2S) glycosidic bond [17]. In the presence of GHK, the A3 resonance is displaced upfield over the entire pD range of 2–10, with the maximum displacement being ~0.16 ppm at pD 6. Other A ring resonances also shift upfield but the shifts are smaller (0.03 and 0.04 ppm for the A1 and A4 resonances at pD 6). The displacement of the A3 resonance is consistent with site-specific binding of the imidazolium group to a binding site in which the imidazolium ring is located above the A3 proton [17], causing the A3 resonance to be shifted upfield by ring current effects [19].

As the pD is increased from 4 to 10, the imidazolium and glycyl ammonium groups are titrated and resonances for the His-C2H and Gly-CH_2 protons shift upfield. In the presence of heparin, the chemical shift titration curves for both are displaced to higher pD. Displacement of the His-C2H chemical shift titration curve to higher pD provides further evidence for participation of the imidazolium group in heparin-GHK binding, while the shift of the Hep-A3 resonance back to the chemical shift of free heparin upon titration of the imidazolium group indicates that only the imidazolium form of the histidyl side-chain is involved in binding. The His-C2H and Gly-CH_2 chemical shift titration curves together with displacement of the Lys ε-CH_2 resonance to lower field (Fig. 3) indicate that the imidazolium, glycyl ammonium and lysine ammonium groups are all involved in binding to heparin at pD 6.

At pD $\geq$ 10, the chemical shifts of the Hep-A3, His-C2H, Gly-CH_2 and Lys ε-CH_2 resonances are the same for solutions containing heparin, GHK and heparin plus GHK, indicating that, even though the lysine side-chain is protonated at pD 10, the (Im, $GlyNH_2$, $LysNH_3^+$) form of GHK does not bind to heparin.

Similar chemical shift titration data were obtained for solutions which contained heparin and GHK at ~5:1 ratio (12.3 mM heparin, 2.6 mM GHK and ~50 mM Na^+ from the sodium heparinate) whereas the displacement of the His-C2H and Gly-CH_2 titration curves to higher pD was somewhat less when solutions also contained 0.15 M NaCl. The dependence on NaCl concentration indicates that binding of GHK involves displacement of Na^+ ions from the polyelectrolyte counterion condensation volume [20] around heparin.

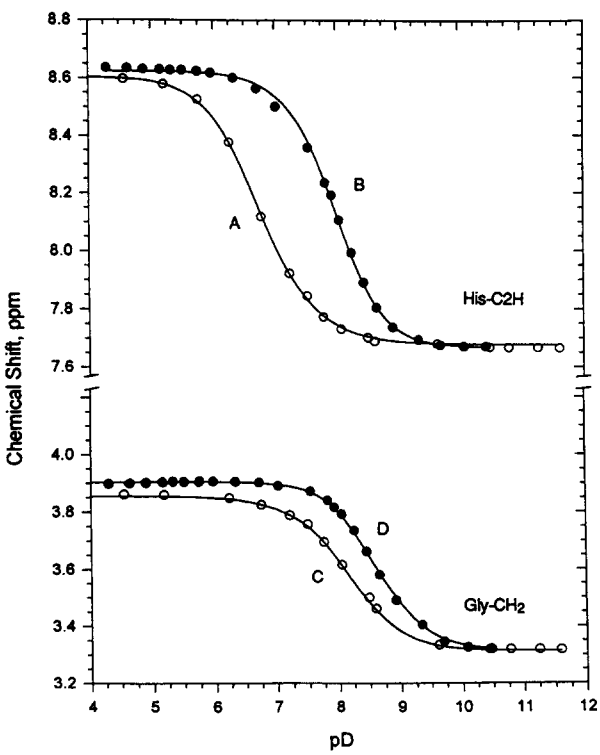

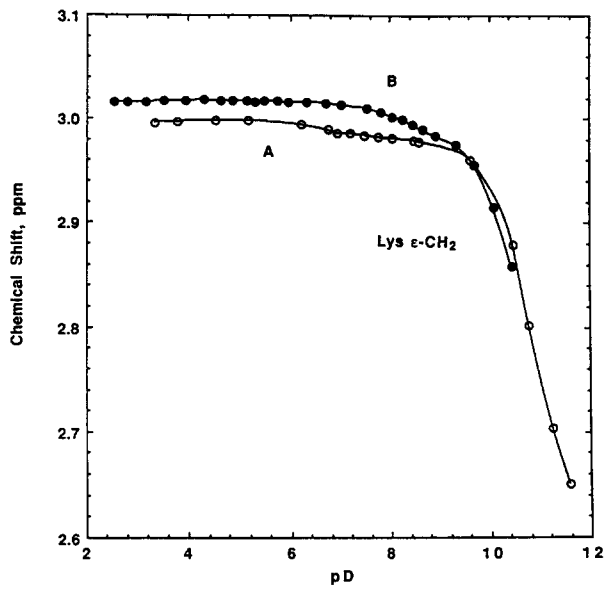

Fig. 3. Chemical shift of the resonance for the Lys ε-CH_2 proton of GHK as a function of pD. Curve A is for 2.6 mM GHK; curve B is for 13.7 mM sodium heparinate + 5.1 mM GHK.

The acid/base and heparin-binding equilibria of GHK are summarized in Fig. 5. The chemical shift data in Fig. 2 indicate that the imidazolium and glycyl ammonium groups of the (ImH^+, $GlyNH_3^+$, $LysNH_3^+$) form of GHK (species A in Fig. 5) are of similar acidity and deprotonate to give either species B or C, which then deprotonate to give species D [21]. Microscopic acid dissociation constants were calculated by fitting the His-C2H and Gly-CH_2 chemical shift data for free GHK in Fig. 2 to Eqns. 3 and 4.

$$\delta_{C2H} = (f_A + f_C)\,\delta_{C2H,ImH} + (f_B + f_D)\,\delta_{C2H,Im} \quad (3)$$

$$\delta_{Gly} = (f_A + f_B)\,\delta_{Gly,NH_3} + (f_C + f_D)\,\delta_{Gly,NH_2} \quad (4)$$

where δ_{C2H} is the observed chemical shift of the His-C2H proton and $\delta_{C2H,ImH}$ and $\delta_{C2H,Im}$ the chemical shifts of the His-C2H proton when the histidine side-chain is in the imidazolium and imidazole forms. δ_{Gly}, δ_{Gly,NH_3} and δ_{Gly,NH_2} are defined analogously for the glycine methylene protons. f_A–f_D are the fractional concentrations of species A–D, as defined in Fig. 5. $f_A = [H^+]^2/Denom$, $f_B = [H^+]k_1/Denom$, $f_C = [H^+]k_2/Denom$ and $f_D = k_1k_{12}/Denom$, where $Denom = [H^+]^2 + [H^+]k_1 + [H^+]k_2 + k_1k_{12}$. Values of $pk_1 = 6.70$, $pk_2 = 7.81$, $pk_{12} = 8.16$ and $pk_{21} = 7.04$ were obtained by fitting simultaneously chemical shift data for the His-C2H and Gly-CH_2 protons by non-linear least squares methods to Eqns. 3 and 4. The solid curves through data sets A and C in Fig. 2 are theoretical curves predicted using these pk values.

The chemical shift data also indicate that GHK species A–C in Fig. 4 interact with heparin. The length of heparin polymer which binds GHK is not known, however, molecular models suggest a tetrasaccharide segment would accomodate one molecule of GHK. Binding constants defined in terms of heparin tetrasaccharide-binding units were estimated by fitting the observed chemical shift data for the His-C2H and Gly-CH_2 protons in the presence of heparin to Eqns. 5 and 6.

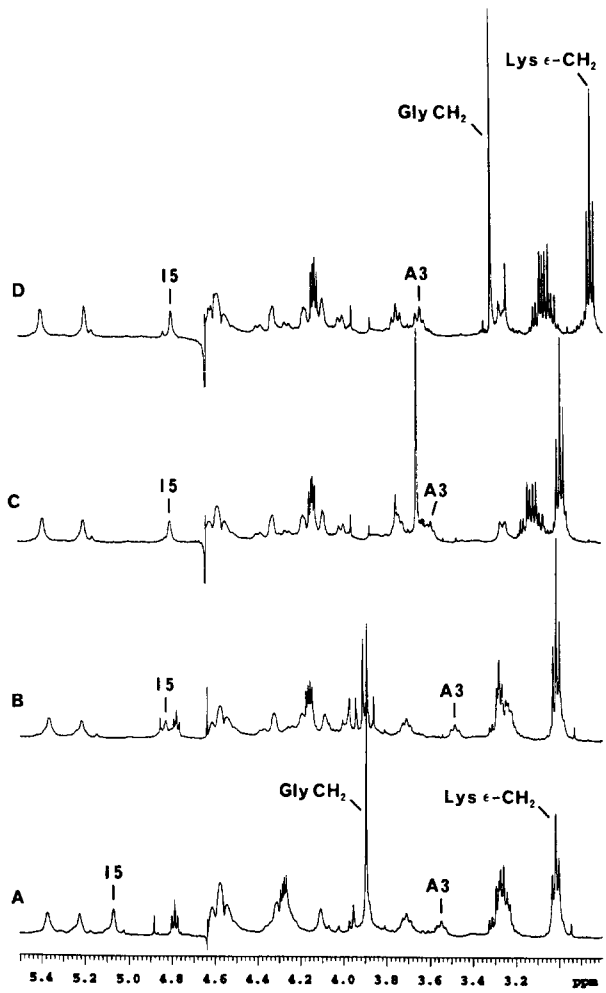

Fig. 4. Portions of the 500 MHz [^{1}H]NMR spectra of a solution which contained 13.7 mM sodium heparinate + 5.1 mM GHK at pD values of (A) 3.93, (B) 6.32, (C) 8.45 and (D) 10.44.

$$\delta_{C2H} = (f_A + f_C)\delta_{C2H,ImH} + (f_B + f_D + f_{Hep\text{-}B})\delta_{C2H,Im} + (f_{Hep\text{-}A} + f_{Hep\text{-}C})\delta_{C2H,Bound} \quad (5)$$

$$\delta_{Gly} = (f_A + f_B)\delta_{Gly,NH_3} + (f_C + f_D + f_{Hep\text{-}C})\delta_{Gly,NH_2} + (f_{Hep\text{-}A} + f_{Hep\text{-}B})\delta_{Gly,Bound} \quad (6)$$

where δ_{C2H} is the observed chemical shift of the His-C2H proton, $\delta_{C2H,ImH}$ and $\delta_{C2H,Im}$ are defined as for Eqn. 3 and $\delta_{C2H,Bound}$ is the chemical shift of the C2H proton of the bound histidine side-chain in the imidizolium form. δ_{Gly}, δ_{Gly,NH_3}, δ_{Gly,NH_2} and $\delta_{Gly,Bound}$ are defined analogously for the glycine methylene protons. f_A, f_B, etc., the fractional concentrations of the subscripted species defined in Fig. 5, were expressed in terms of the microscopic acid dissociation constants, the binding constants and the concentrations of GHK and heparin tetrasaccharide. Values of $K_{f1} = 12{,}700 \pm 300$ M, $K_{f2} = 250 \pm 20$ M, and $K_{f3} = 300 \pm 90$ M were estimated for the binding constants by fitting simultaneously data sets B and D in Fig. 2 to Eqns. 5 and 6. Binding constants of $K_{f1} = 36{,}500 \pm 1300$ M, $K_{f2} = 480 \pm 30$ M and $K_{f3} = 500 \pm 150$ M were estimated using data sets analogous to B and D in Fig. 2 for 2.6 mM GHK plus 12.3 mM heparin disaccharide. The decrease in binding constant as the heparin to peptide ratio decreases indicates anticooperativity in the binding of GHK. The solid curves through data sets B and D in Fig. 2 are theoretical curves calculated using the microscopic acid dissociation constants and the binding constants estimated from these data sets. The distribution of GHK among its various protonated and heparin-bound species is shown as a function of pD in Fig. 6.

3.1. Conclusions

The chemical shift data presented in Figs. 1–3 establish that the growth factor GHK can bind to heparin, and presumably also to the heparin-like $[(IdoA\text{-}2S)\text{-}(1\rightarrow4)\text{-}GlcNSO_3\text{-}6S)]_n$ sequences of cell surface heparan sulfate proteoglycans [15,16]. The nature of the heparin–GHK binding interaction is pH-dependent. At low pH, where the heparin carboxylate group is protonated, the binding involves delocalized electrostatic interactions between cationic GHK and anionic heparin. At physiological pH, the imidazolium side-chains of the (ImH^+, $GlyNH_3^+$, $LysNH_3^+$) form of GHK bind site specifically to imidazolium-binding sites on heparin, while the ammonium groups interact with heparin carboxylate groups. The species distribution diagram in Fig. 6 shows that the extent and nature of the binding are sensitive to pH, with a significant amount of heparin binding to the (ImH^+, $GlyNH_3^+$, $LysNH_3^+$) and (Im, $GlyNH_3^+$, $LysNH_3^+$) forms of GHK at physiological pH.

The basic side-chains of lysine and arginine are generally assumed to be the sites of heparin and heparan sulfate binding to proteins [22], although it has been suggested that the histidine side-chains of several peptides and proteins, including synthetic β-amyloid peptides [23], histidine-rich glycoprotein [24] and platelet factor 4 [25], bind to heparin. The results presented

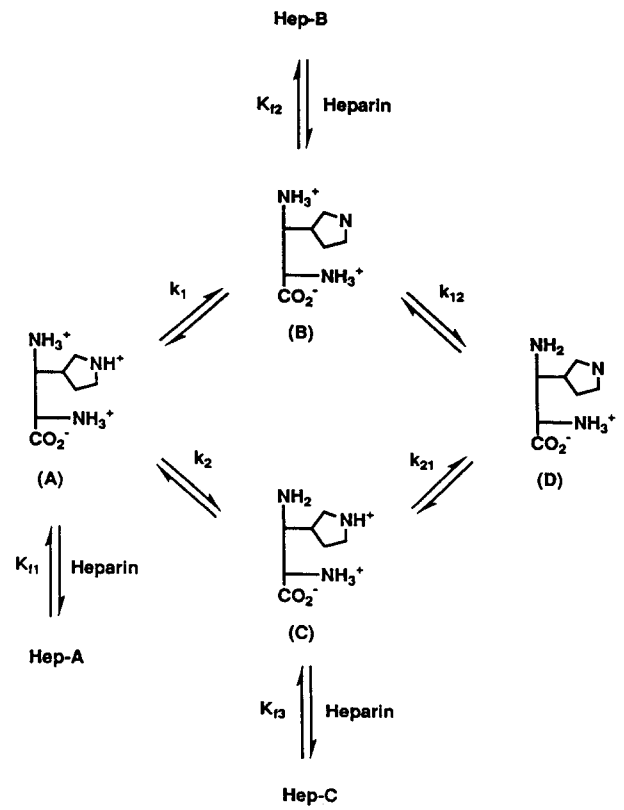

Fig. 5. Microscopic acid dissociation and heparin-binding scheme for GHK.

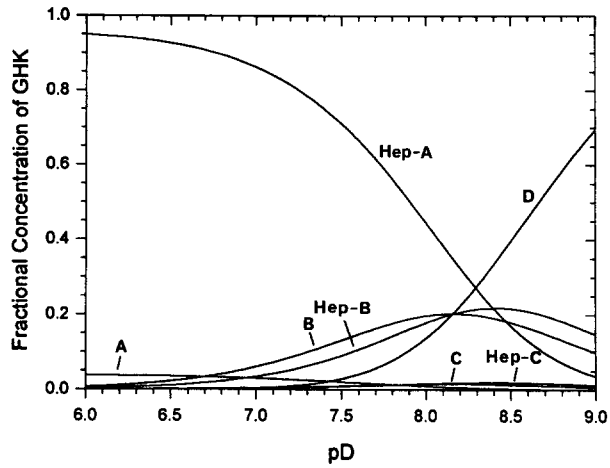

Fig. 6. Species distribution of GHK in a solution containing total peptide and heparin concentrations of 5.1 mM and 13.7 mM, respectively. The species are defined in Fig. 5. The distribution curves were calculated using equations which express the fractional concentrations in terms of the microscopic acid dissociation constants, the binding constants (K_{f1} = 12,700, K_{f2} = 250 and K_{f3} = 300) and the concentration of peptide and heparin.

here provide direct experimental evidence for heparin-histidine side-chain binding.

Acknowledgements: This research was supported in part by National Institutes of Health Grant AI 24216.

References

[1] Pickart, L. and Thaler, M.M. (1973) Nature New Biol. 243, 85–87.
[2] Pickart, L. and Lovejoy, S. (1987) Methods Enzymol. 147, 314–328.
[3] Sensenbrenner, M., Jaros, G.G., Moonen, G. and Mandel, P. (1975) Neurobiology 5, 207–213.
[4] Sensenbrenner, M., Jaros, G.G., Moonen, G. and Meyer, B.J. (1980) Experientia 36, 660–662.
[5] Hague, A. and Capron, A. (1982) Nature (London) 299, 361–363.
[6] Pickart, L., Thayer, L. and Thaler, M.M. (1973) Biochem. Biophys. Res. Commun. 54, 562–566.
[7] Stromberg, B.E., Khoury, P.B. and Soulsby, E.J.L. (1977) Int. J. Parasitol. 7, 149–151.
[8] Stromberg, B.E. (1979) Int. J. Parasitol. 9, 307–311.
[9] Nelson, P.D., Weiner, D.J., Stromberg, B.E. and Abraham, D. (1982) J. Parasitol. 68, 971–973.
[10] Williams, M.V. and Cheng, Y. (1980) Cytobios 27, 19–25.
[11] Poole, T. and Zetter, B. (1983) Cancer Res. 43, 5857–5861.
[12] Zetter, B., Rasmussen, N. and Brown, L. (1985) Lab. Invest. 53, 362–368.
[13] Wegrowski, Y., Maquart, F.X. and Borel, J.P. (1992) Life Sci. 51, 1049–1056.
[14] Maquart, F.X., Bellon, G. Chaqour, B., Wegrowski, J., Patt, L.M., Trachy, R.E., Monboisse, J.C., Chastang, F., Birembaut, P., Gillery, P. and Borel, J.P. (1993) J. Clin. Invest. 92, 2368–2376.
[15] Lindahl, U., Lidholt, K., Spillmann, D. and Kjellen, L. (1994) Thrombosis Res. 75, 1–32.
[16] Gallagher, J.T. (1986) Nature (London) 326, 136.
[17] Rabenstein, D.L., Bratt, P., Schierling, T.D., Robert, J.M. and Guo, W. (1992) J. Am. Chem. Soc. 114, 3278–3285.
[18] Glasoe, P.K. and Long, F.A. (1960) J. Phys. Chem. 64, 188–190.
[19] Wuthrich, K. (1986) NMR of Proteins and Nucleic Acids, John Wiley, New York, NY.
[20] Manning, G.S. (1978) Q. Rev. Biophys. 11, 179–246.
[21] Rabenstein, D.L., Greenberg, M.S. and Evans, C.A. (1977) Biochemistry 16, 977–981.
[22] Cardin, A.D. and Weintraub, H.J.R. (1989) Arteriosclerosis 9, 21–32.
[23] Brunden, K.R., Richter-Cook, N.J., Chaturvedi, N. and Frederickson, R.C.A. (1993) J. Neurochem. 61, 2147–2154.
[24] Burch, M.K., Blackburn, M.N. and Morgan, W.T. (1987) Biochemistry 26, 7477–7482.
[25] Talpas, C.J. and Lee, L. (1993) J. Protein Chem. 12, 303–309.